

Highly efficient and stable inverted bottom-emission organic light emitting devices

Ta-Ya Chu, Jenn-Fang Chen, Szu-Yi Chen, Chao-Jung Chen, and Chin H. Chen

Citation: *Applied Physics Letters* **89**, 053503 (2006); doi: 10.1063/1.2268923

View online: <http://dx.doi.org/10.1063/1.2268923>

View Table of Contents: <http://scitation.aip.org/content/aip/journal/apl/89/5?ver=pdfcov>

Published by the [AIP Publishing](#)

Articles you may be interested in

[A soluble nonionic surfactant as electron injection material for high-efficiency inverted bottom-emission organic light emitting diodes](#)

Appl. Phys. Lett. **93**, 123310 (2008); 10.1063/1.2982586

[Cesium hydroxide doped tris-\(8-hydroxyquinoline\) aluminum as an effective electron injection layer in inverted bottom-emission organic light emitting diodes](#)

Appl. Phys. Lett. **92**, 263305 (2008); 10.1063/1.2955516

[Double interfacial layers for highly efficient organic light-emitting devices](#)

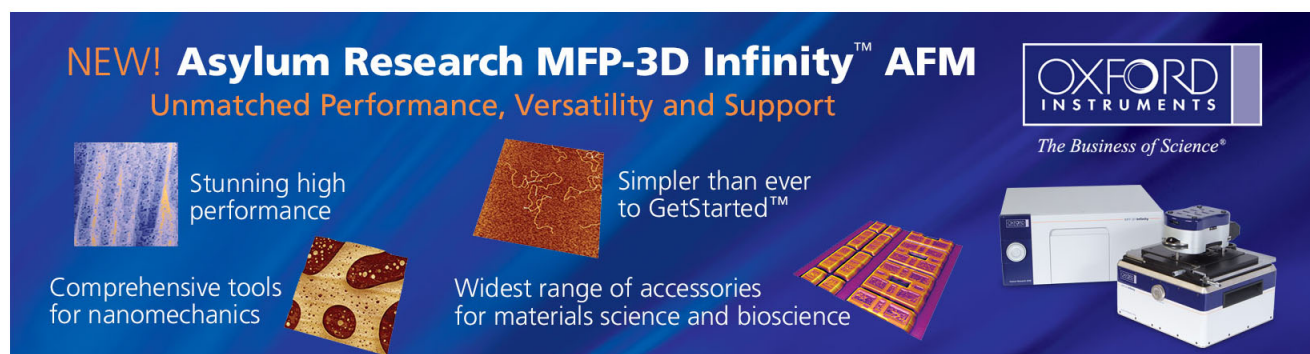
Appl. Phys. Lett. **90**, 153508 (2007); 10.1063/1.2721872

[High efficiency red organic light-emitting devices using tetraphenyldibenzoperiflanthene-doped rubrene as an emitting layer](#)

Appl. Phys. Lett. **89**, 013502 (2006); 10.1063/1.2218833

[Effective intermediate layers for highly efficient stacked organic light-emitting devices](#)

Appl. Phys. Lett. **87**, 093504 (2005); 10.1063/1.2035320

The advertisement features a dark blue background with white and orange text. At the top left, it reads 'NEW! Asylum Research MFP-3D Infinity™ AFM' in large white letters, followed by 'Unmatched Performance, Versatility and Support' in orange. To the right is the Oxford Instruments logo, which includes the text 'OXFORD INSTRUMENTS' and the tagline 'The Business of Science®'. Below the main text are four images: a textured surface, a circular pattern, a grid of small squares, and the AFM instrument itself. Each image is accompanied by a short text description: 'Stunning high performance', 'Simpler than ever to GetStarted™', 'Comprehensive tools for nanomechanics', and 'Widest range of accessories for materials science and bioscience'.

Highly efficient and stable inverted bottom-emission organic light emitting devices

Ta-Ya Chu^{a)} and Jenn-Fang Chen

Institute of Electrophysics, National Chiao Tung University, Hsinchu 300, Taiwan

Szu-Yi Chen and Chao-Jung Chen

Display Institute, National Chiao Tung University, Hsinchu 300, Taiwan

Chin H. Chen

Display Institute, National Chiao Tung University, Hsinchu 300, Taiwan and Microelectronics and Information Systems Research Center, National Chiao Tung University, Hsinchu 300, Taiwan

(Received 28 March 2006; accepted 29 June 2006; published online 1 August 2006)

The authors report the development of highly efficient and stable C545T doped green fluorescent Alq₃ inverted bottom-emission organic light emitting device (IOLED), with a device configuration of ITO/Mg/Cs₂O:Bphen/Alq₃/C545T:Alq₃/NPB/WO₃/Al, that achieved a maximum current efficiency of 23.7 cd/A and a power efficiency of 12.4 lm/W which are two times better than those of the conventional OLED. At a brightness level of 100 cd/m², the device required driving current density only as low as 0.5 mA/cm² at a driving voltage of only 5.0 V and its half-lifetime $T_{1/2}$ in excess of 104 000 h. © 2006 American Institute of Physics. [DOI: 10.1063/1.2268923]

Active-matrix organic light emitting device (AMOLED) has the potential to become one of the major flat panel displays of the future. Low-temperature polycrystalline silicon (LTPS) and amorphous silicon (*a*-Si) thin film transistor (TFT) backplane technologies are currently used in AMOLED. Recent consumer products such as the BenQ-Siemens S88 2 in. mobile display camera and the Sony CLIE PEG-VZ90 3.8 in. personal digital assistant (PDA) have used LTPS TFT as the backplane for their OLED displays. This is because LTPS has higher carrier mobility than *a*-Si and both *n*- and *p*-type TFTs can be fabricated on LTPS. Hence, a *p*-type TFT can be used as the driving TFT in an AMOLED, and the bottom anode of a conventional OLED can be positioned at the drain end of the *p*-type TFT. It is also true that the decay of luminance in AMOLED fabricated on a LTPS TFT backplane is much lower than that fabricated on an *a*-Si backplane with a conventional OLED. However, as LTPS not only requires more masks than the *a*-Si process but also is limited by the size of the available substrate, LTPS-TFT OLED would be difficult to compete with the robust *a*-Si-based technology particularly in large sized displays such as TV in manufacturing cost as well as in yield.

Therefore, there is growing interest and demand in the OLED community to develop technology that can adapt to the *a*-Si TFT backplane. Since only *n*-channel TFT can be used in *a*-Si backplanes, conventional OLED with bottom anode can only be fabricated at the source end of the driving *a*-Si TFT, which would impact on the stability of the source voltage that depends on the voltage drop across the OLED materials.

Several researchers have opted instead to use Al, a reflective metal, as bottom cathode and have tried to sputter transparent indium tin oxide (ITO) on organic layers to fabricate inverted top-emission OLEDs (ITOLEDs).¹⁻⁵ However, the sputter deposition of ITO is known to induce radia-

tion damage to the organic layers.⁶ Other authors have used a semitransparent film of Au (10–20 nm),^{7,8} NiO,⁹ indium zinc oxide,¹⁰ or Ag/TeO₂,¹¹ as the top anode of ITOLED. But, the variation of electroluminescence (EL) spectra at different viewing angles caused by microcavity effect induced by the two opposite reflective metal/semitransparent metal electrodes somehow limits the advantage of this approach.¹² Leo and co-workers reported the transparent inverted *p-i-n* OLED,¹³⁻¹⁵ where Au was used as the top anode.

From all things considered, the most direct way to alleviate this problem would be to use an inverted OLED (IOLED) for *n*-channel TFT because IOLED has a bottom cathode that can be connected directly to a TFT, which is located at the drain end of *a*-Si TFT. Both the gate and the source voltages of the driving *a*-Si TFT are directed through the gate and the data lines thus independent of the IOLED materials.

We have developed highly efficient and stable green fluorescent dye-doped IOLED which achieved luminescence efficiencies of 23.7 cd/A and power efficiency of 12.4 lm/W. Figure 1 compares the structure of our IOLED with that of a conventional OLED with a bottom anode. We will show that this high efficiency is not due to microcavity effect of the inverted structure. To the best of our knowledge, the performances are among the best ever reported for an

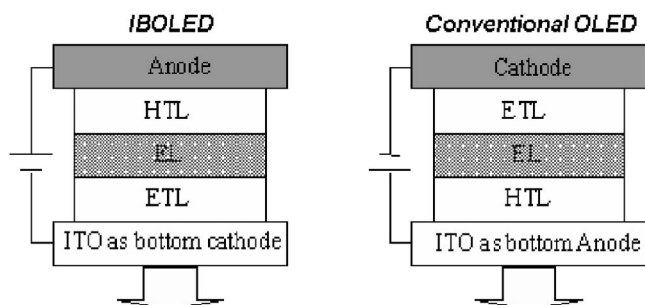


FIG. 1. Schematic illustration of the IOLED and conventional OLED structures.

^{a)} Author to whom correspondence should be addressed; electronic mail: tayachu@gmail.com

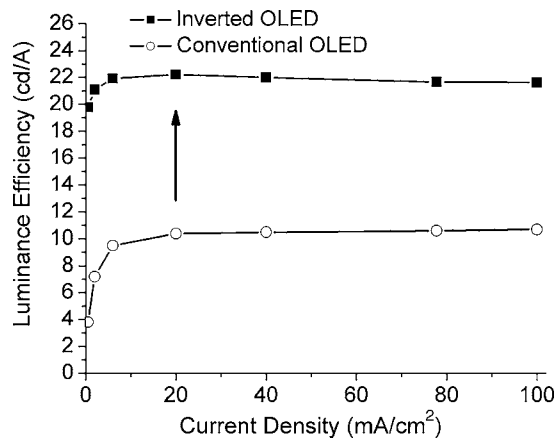


FIG. 2. Luminance efficiency-current density characteristics of an IBOLED vs conventional OLED.

inverted OLED. We believe that the inverted OLEDs developed in this work can be integrated with *a*-Si TFT process that would considerably accelerate the commercialization of large size AMOLEDs of the future.

The most commonly used green fluorescent emitting layers in OLED are Alq₃ doped with about 1% 10-(2-benzothiazolyl)-2,3,6,7-tetrahydro-1,1,7,7-tetra(methyl)-1*H*,5*H*,11*H*-[1]-benzopyrano [6,7,8-*ij*]quinolizin-11-one (C545T). The conventional OLED structure employed in this study was ITO(anode)/CuPc(15 nm)/NPB(60 nm)/C545T:Alq₃(37.5 nm)/Alq₃(37.5 nm)/LiF(1 nm)/Al, which has a luminance efficiency of 10.4 cd/A at 20 mA/cm². The same host and guest emitter were likewise fabricated in the IBOLED whose device structure was ITO(cathode)/Mg(1 nm)/Cs₂O:Bphen(11 nm)/Alq₃(30 nm)/C545T:Alq₃(30 nm)/NPB(60 nm)/WO₃(5 nm)/Al. The electron injection material which was composed of bilayer Mg/Cs₂O: 4,7-diphenyl-1,10-phenanthroline (Bphen) was used as electron injection layer.^{16,17} The evaporate of WO₃ is employed as the hole injection layer.¹⁸ The EL of the devices was characterized using a diode array rapid scanning system that included a Photo Research PR650 spectrophotometer and a computer controlled programmable dc source. Figure 2 compares the luminance-current density (*L*-*J*) characteristics of the IBOLED with those of the conventional OLEDs. The luminance efficiency of our IBOLED of 22.2 cd/A at 20 mA/cm² is two times better than that of the conventional OLED with 10.4 cd/A.

Figure 3(a) plots the current density-voltage-luminance (*J*-*V*-*L*) characteristics of the C545T doped green fluorescent IBOLED. The threshold voltage is around 3.0 V. A brightness of 4450 cd/m² and its maximum of 106 800 cd/m² are achieved at 20 and 450 mA/cm², respectively. Figure 3(b) plots the power and current efficiencies against luminance of IBOLED. The maximum power efficiency of IBOLED is found at 12.4 lm/W while the luminance efficiency is 19.8 cd/A. The IBOLED with a luminance of 100 cd/m² required only a current density as low as 0.5 mA/cm² at a driving voltage of only 5.0 V. The device is capable of achieving an external quantum efficiency of 6% and a maximum luminance efficiency of 23.7 cd/A. Recently, Sun *et al.*¹⁹ fabricated two unit stacked OLEDs (SOLEDs) using the intermediate layers of LiF/Ca/Ag to get high efficiency of 19.6 cd/A based on the emission of C545T. However, stacked OLED structure tends to cause considerable color

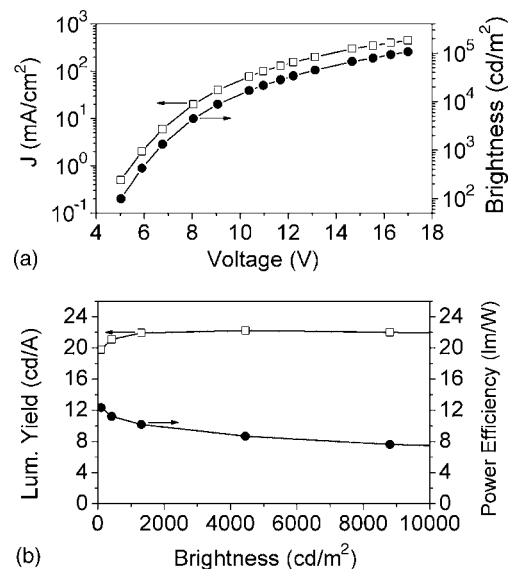


FIG. 3. (a) Current density-voltage-luminance (b) Power efficiency vs luminance vs luminance efficiency characteristics for the green emission (C545T:Alq₃) of IBOLED.

deviation at different viewing angles due to the intrinsic microcavity effect. On the contrary, we have measured the electroluminescence spectra with relative intensities at different view angles, as shown in Fig. 4. We did not observe any color change with respect to viewing angles, which means the high efficiency of IBOLED is not due to microcavity effect enhancement as often observed in top-emission OLEDs (Ref. 12) or SOLED.

The measurements of the lifetime of the device were made in a glovebox at constant driving current densities of 15 mA/cm² (3300 cd/m²) and 33 mA/cm² (7200 cd/m²), respectively. Figure 5 shows the device operational stability of IBOLED. The lifetime was extrapolated according to

$$L_0^n \times T_{1/2} = \text{const},$$

where L_0 is the luminance, $T_{1/2}$ is the time needed for the luminance to decrease to 50% of the initial value, and n is an acceleration exponent.²⁰ The acceleration factor (n) of IBOLED has been estimated to be about 1.47, as depicted in Fig. 5(b). Therefore, the lifetime of the green fluorescent

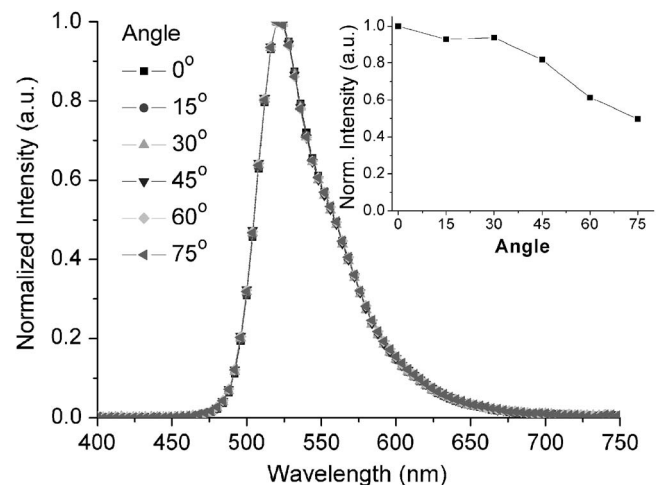


FIG. 4. Measured EL spectra with relative intensities (inset) at 0°-75° off the surface normal of the IBOLED.

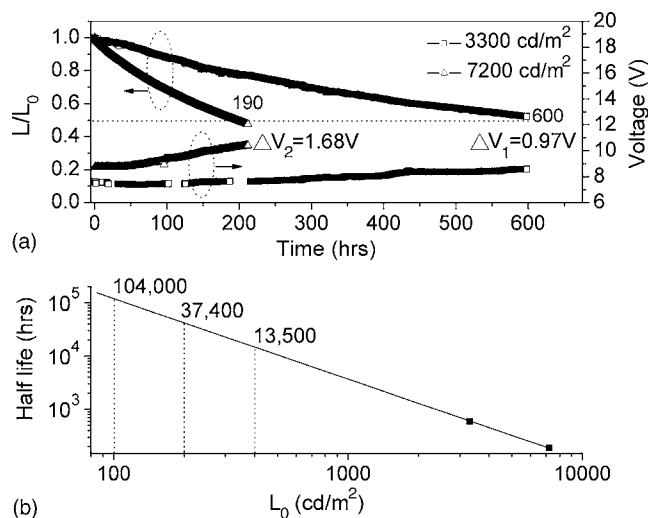


FIG. 5. (a) Stabilities of luminance decreasing and voltage increasing were measured at initial luminance of 3300 and 7200 cd/m^2 , respectively. (b) Estimated half-life with fitted acceleration coefficient of $n=1.47$.

dye-doped (C545T:Alq₃) IBOLED is extrapolated to be over 104 000 h at a normalized initial luminance of 100 cd/m^2 while the conventional green OLED has a lifetime of only 57 000 h assuming the same of acceleration factor. Furthermore, the voltage increasing with continuous operation of the device driven at constant current of 15 mA/cm^2 was only 0.97 V after 600 h. This stability result appears to suggest that our IBOLED structure actually can enhance the stability of the device.

In summary, we report the highly efficient doped green fluorescent (23.7 cd/A , 12.4 lm/W) IBOLED based on the ITO/Mg/Cs₂O:Bphen bottom cathode and WO₃/Al top anode that are more efficient than those of the conventional bottom-emission OLEDs. A brightness of 100 cd/m^2 of IBOLED requires a current density of as low as 0.5 mA/cm^2 at only 5.0 V. We believe that this performance is among the best ever reported in the literature for the inverted OLEDs. The C545T doped green fluorescent device also has a projected half-decay ($t_{1/2}$) lifetime of more than 100 000 h at an initial luminance of 100 cd/m^2 which is 50% better than that of the conventional OLED. Although the disadvantages of IBOLED similar to conventional bottom-emission OLEDs are its smaller aperture ratio, we believe that the IBOLED structure described in this study which can be integrated

readily with the n channel of the a -Si TFT backplane will prove useful in manufacturing AMOLED with high power efficiency and long device stability for future large-size OLED display applications.

This work was supported by grants from Chunghwa Picture Tubes, Ltd. of Taoyuan, Taiwan, which also generously provided a scholarship for two of the authors (T.-Y.C. and S.-Y.C.) at NCTU. The authors thank e-Ray Optoelectronics Technology Co., Ltd. of Taiwan for generously supplying some of the OLED materials studied in this work.

¹W. Kowalsky, E. Becker, T. Benstem, H.-H. Johannes, D. Metzdorf, H. Zeuner, and J. Schobel, Proc. SPIE **4105**, 194 (2001).

²T. Dobbertin, O. Werner, J. Meyer, A. Kammoun, D. Schneider, T. Riedl, E. Becker, H. H. Johannes, and W. Kowalsky, Appl. Phys. Lett. **83**, 5071 (2003).

³S. Kho, S. Sohn, and D. Jung, Jpn. J. Appl. Phys., Part 2 **42**, L552 (2003).

⁴J. M. Zhao, Y. Q. Zhan, S. T. Zhang, X. J. Wang, Y. C. Zhou, Y. Wu, Z. J. Wang, X. M. Ding, and X. Y. Hou, Appl. Phys. Lett. **84**, 5377 (2004).

⁵S. Kho, S. Sohn, and D. Jung, J. Korean Phys. Soc. **46**, 1224 (2005).

⁶L. S. Liao, L. S. Hung, W. C. Chan, X. M. Ding, T. K. Sham, I. Bello, C. S. Lee, and S. T. Lee, Appl. Phys. Lett. **75**, 1619 (1999).

⁷H. W. Choi, S. Y. Kim, W.-K. Kim, and J.-L. Lee, Appl. Phys. Lett. **87**, 082102 (2005).

⁸L. Hou, F. Huang, W. Zeng, J. Peng, and Y. Cao, Appl. Phys. Lett. **87**, 153509 (2005).

⁹S.-W. Park, J.-M. Choi, E. Kim, and S. Im, Appl. Surf. Sci. **244**, 439 (2005).

¹⁰T. Miyashita, S. Naka, H. Okada, and H. Onnagawa, Proceedings IDW'04 (2004), p. 1421.

¹¹C.-W. Chen, C.-L. Lin, and C.-C. Wu, Appl. Phys. Lett. **85**, 2469 (2004).

¹²X. Zhu, J. Sun, H. Peng, M. Wong, and H.-S. Kwok, SID Int. Symp. Digest Tech. Papers **2005**, 793.

¹³S. Huang, J. Blochwitz-Nimoth, D. S. Qin, A. Wemer, J. Drechsel, B. Maennig, and K. Leo, Appl. Phys. Lett. **81**, 922 (2002).

¹⁴X. Zhou, J. Blochwitz-Nimoth, M. Pfeiffer, B. Maennig, J. Drechsel, A. Werner, and K. Leo, Synth. Met. **138**, 193 (2003).

¹⁵J. B. Nimoth, J. Brandt, M. Hofmann, J. Birnstock, M. Pfeiffer, G. He, P. Wellmann, and K. Leo, SID Int. Symp. Digest Tech. Papers **2004**, 1003.

¹⁶T.-Y. Chu, S.-Y. Chen, J.-F. Chen, and C.-H. Chen, Jpn. J. Appl. Phys., Part 1 **45**, 4948 (2006).

¹⁷T.-Y. Chu, S.-Y. Chen, J.-F. Chen, and C.-H. Chen, Appl. Phys. Lett. (to be published).

¹⁸J. Li, M. Yahiro, K. Ishida, H. Yamada, and K. Matsushige, Synth. Met. **151**, 141 (2005).

¹⁹J. X. Sun, X. L. Zhu, H. J. Peng, M. Wong, and H. S. Kwok, Appl. Phys. Lett. **87**, 093504 (2005).

²⁰P. Wellmann, M. Hofmann, O. Zeika, A. Werner, J. Birnstock, R. Meerheim, G. He, K. Walzer, M. Pfeiffer, and K. Leo, SID Int. Symp. Digest Tech. Papers **2005**, 393.